



Characterization of the Plasmidome Encoding Carbapenemase and Mechanisms for Dissemination of Carbapenem-Resistant *Enterobacteriaceae*

Ryuichiro Abe,^{a,b}  Yukihiro Akeda,^{a,c,d}  Yo Sugawara,^a Dan Takeuchi,^a Yuki Matsumoto,^e Daisuke Motooka,^e Norihisa Yamamoto,^{a,b,c} Ryuji Kawahara,^f Kazunori Tomono,^{c,d} Yuji Fujino,^b Shigeyuki Hamada^a

^aJapan-Thailand Research Collaboration Centre on Emerging and Re-emerging Infections, Research Institute for Microbial Diseases, Osaka University, Osaka, Japan

^bDepartment of Anaesthesiology and Intensive Care Medicine, Graduate School of Medicine, Osaka University, Osaka, Japan

^cDivision of Infection Control and Prevention, Osaka University Hospital, Osaka, Japan

^dDivision of Infection Control and Prevention, Graduate School of Medicine, Osaka University, Osaka, Japan

^eDepartment of Infection Metagenomics, Research Institute for Microbial Diseases, Osaka University, Osaka, Japan

^fDepartment of Microbiology, Osaka Institute of Public Health, Osaka, Japan

ABSTRACT Carbapenem-resistant *Enterobacteriaceae* (CRE) infections, high in morbidity and mortality, pose serious clinical challenges due to limited treatment options. A previous CRE surveillance study on 1,507 patients from 43 hospitals in Osaka, Japan, revealed that 12% of patients carried CRE and that 95% of the CRE isolates were IMP-type carbapenemase producers. Here, the mechanisms for this regional dissemination of a single carbapenemase gene were investigated. Since the dissemination of CRE is primarily due to the transmission of carbapenemase genes located on plasmids, we analyzed the plasmidome of 230 CRE isolates carrying *bla*_{IMP} by whole-genome sequencing and Southern blotting. *bla*_{IMP-6} was found to be predominantly disseminated among chromosomally distinct isolates through the pKPI-6 plasmid. Underlying the vast clonal dissemination of pKPI-6, various subpopulations deriving from pKPI-6 were identified, which had acquired advantages for the dissemination of CRE isolates. A cluster exhibiting heteroresistance against meropenem by the transcriptional regulation of *bla*_{IMP-6} caused an outbreak likely through covert transmission of *bla*_{IMP-6}. For stable carriage of *bla*_{IMP-6}, they occasionally integrated *bla*_{IMP-6} on their chromosomes. In addition, we detected one isolate that broadened the range of antimicrobial resistance through a single point mutation in *bla*_{IMP-6} on pKPI-6. Multifaceted analysis of the plasmidome granted us more accurate perspectives on the horizontal spread of CRE isolates, which is difficult to trace only by comparing the whole genomes. This study revealed the predominant spread of a specific carbapenemase-encoding plasmid accompanying the emergence of phenotypically diverse derivatives, which may facilitate further dissemination of CRE in various environments.

IMPORTANCE Global dissemination of carbapenem-resistant *Enterobacteriaceae* (CRE) threatens human health by limiting the efficacy of antibiotics even against common bacterial infections. Carbapenem resistance, mainly due to carbapenemase, is generally encoded on plasmids and is spread across bacterial species by conjugation. Most CRE epidemiological studies have analyzed whole genomes or only contigs of CRE isolates. Here, plasmidome analysis on 230 CRE isolates carrying *bla*_{IMP} was performed to shed light into the dissemination of a single carbapenemase gene in Osaka, Japan. The predominant dissemination of *bla*_{IMP-6} by the pKPI-6 plasmid among genetically distinct isolates was revealed, as well as the emergences of pKPI-6 derivatives that acquired advantages for further disseminations. Underlying vast clonal dissemination of a carbapenemase-encoding plasmid, heteroresistance

Citation Abe R, Akeda Y, Sugawara Y, Takeuchi D, Matsumoto Y, Motooka D, Yamamoto N, Kawahara R, Tomono K, Fujino Y, Hamada S. 2020. Characterization of the plasmidome encoding carbapenemase and mechanisms for dissemination of carbapenem-resistant *Enterobacteriaceae*. *mSystems* 5:e00759-20. <https://doi.org/10.1128/mSystems.00759-20>.

Editor Charles Langelier, UCSF

Copyright © 2020 Abe et al. This is an open-access article distributed under the terms of the [Creative Commons Attribution 4.0 International license](https://creativecommons.org/licenses/by/4.0/).

Address correspondence to Yukihiro Akeda, akeda@biken.osaka-u.ac.jp.

Received 11 August 2020

Accepted 21 October 2020

Published 10 November 2020

was found in CRE offspring, which was generated by the transcriptional regulation of bla_{IMP-6} , stabilization of bla_{IMP-6} through chromosomal integration, or broadened antimicrobial resistance due to a single point mutation in bla_{IMP-6} .

KEYWORDS *Enterobacteriaceae*, IMP-1, IMP-6, carbapenem resistance, carbapenemase, chromosomal integration, heteroresistance, plasmid analysis, plasmid dynamics, plasmidome

The rapid global dissemination of multidrug-resistant *Enterobacteriaceae* threatens health care systems worldwide (1). Carbapenem-resistant *Enterobacteriaceae* (CRE) are of major concern because alternative treatment options are limited (2). Carbapenem resistance is primarily conferred by carbapenemases that hydrolyze carbapenem (3). KPC, NDM, and OXA-48 are the most commonly detected carbapenemases (3). Carbapenemase genes are generally plasmid encoded and are frequently transmitted across species (4). Therefore, genetic tracking of plasmids encoding carbapenemase genes has allowed the monitoring of the spread of CRE isolates. For example, structural similarities among plasmids from isolates obtained in a single hospital outbreak allowed elucidating links between patients carrying the isolates (5–7), and plasmid data accumulated globally revealed the worldwide spread of an epidemic plasmid carrying bla_{KPC} (8). However, most regional surveillance studies compared the whole genomes or only contigs of CRE isolates without analyzing the clonality of the spreading carbapenemase-encoding plasmids, and few studies have comprehensively analyzed carbapenemase-encoding plasmids broadly spreading in a certain region (9).

We previously conducted a surveillance study of CRE in 1,507 patients from 43 hospitals in northern Osaka (population, 1,170,000; area, 307 km²), Japan (10), and we reported that 12% of the patients carried CRE and 95% of CRE isolates harbored bla_{IMP-6} , the predominant carbapenemase in Japan. The predominance of this particular carbapenemase gene might have resulted from vigorous horizontal spreading of a specific plasmid carrying bla_{IMP-6} in this region. The aim of the present study was to analyze the plasmidome transmitting carbapenemase genes in order to unveil the mechanisms for their regional dissemination.

RESULTS

Dissemination of pKPI-6. All bla_{IMP} -positive CRE isolates of *Escherichia coli* ($n = 135$) and *Klebsiella pneumoniae* ($n = 95$) were classified into seven groups based on the results of S1-PFGE followed by Southern blotting hybridization with probes for the bla_{IMP} and $repA$ genes encoded on the IncN-type plasmid pKPI-6, sporadically reported as a plasmid carrying bla_{IMP-6} (11) (Fig. 1). Ninety-nine of the 135 *E. coli* isolates (73%) and 88 of the 95 *K. pneumoniae* isolates (93%) carried plasmids classified as group pKPI-6 based on plasmid size and replicon type (see Fig. S1 in the supplemental material). Next, we compared the similarity between pKPI-6 and 39 representative plasmids categorized as group pKPI-6 based on whole-genome sequencing (WGS) data using Illumina HiSeq 3000 or Illumina MiSeq (see Fig. S1). The overall sequence identity was $99\% \pm 0.28\%$, and the sequence coverage was $98\% \pm 4.0\%$ (mean \pm the standard deviation). The complete sequences of three plasmids were previously confirmed as clonal with pKPI-6 using a combination of PacBio RsII, Illumina HiSeq 3000, and Southern blot methods (12). These analyses confirmed that pKPI-6 was the predominant plasmid responsible for the transmission of bla_{IMP-6} in the study area (187 of 230 [81.3%] bla_{IMP} -positive CRE isolates).

Genomic analysis of derivatives of the predominant plasmid, pKPI-6. During the characterization of the bla_{IMP-6} plasmids mentioned above, nine *E. coli* isolates and three *K. pneumoniae* isolates possessed bla_{IMP-6} plasmids categorized as group IncN (Fig. 1). Group IncN bla_{IMP-6} plasmids were characterized by replicon type IncN and ranged from 35 to 264 kbp in size, which was different from the pKPI-6 plasmid of 50 kbp (see Fig. S1). The complete sequences of these plasmids indicated that they had preserved the nearly complete locus of pKPI-6 and typically were multireplicon plas-

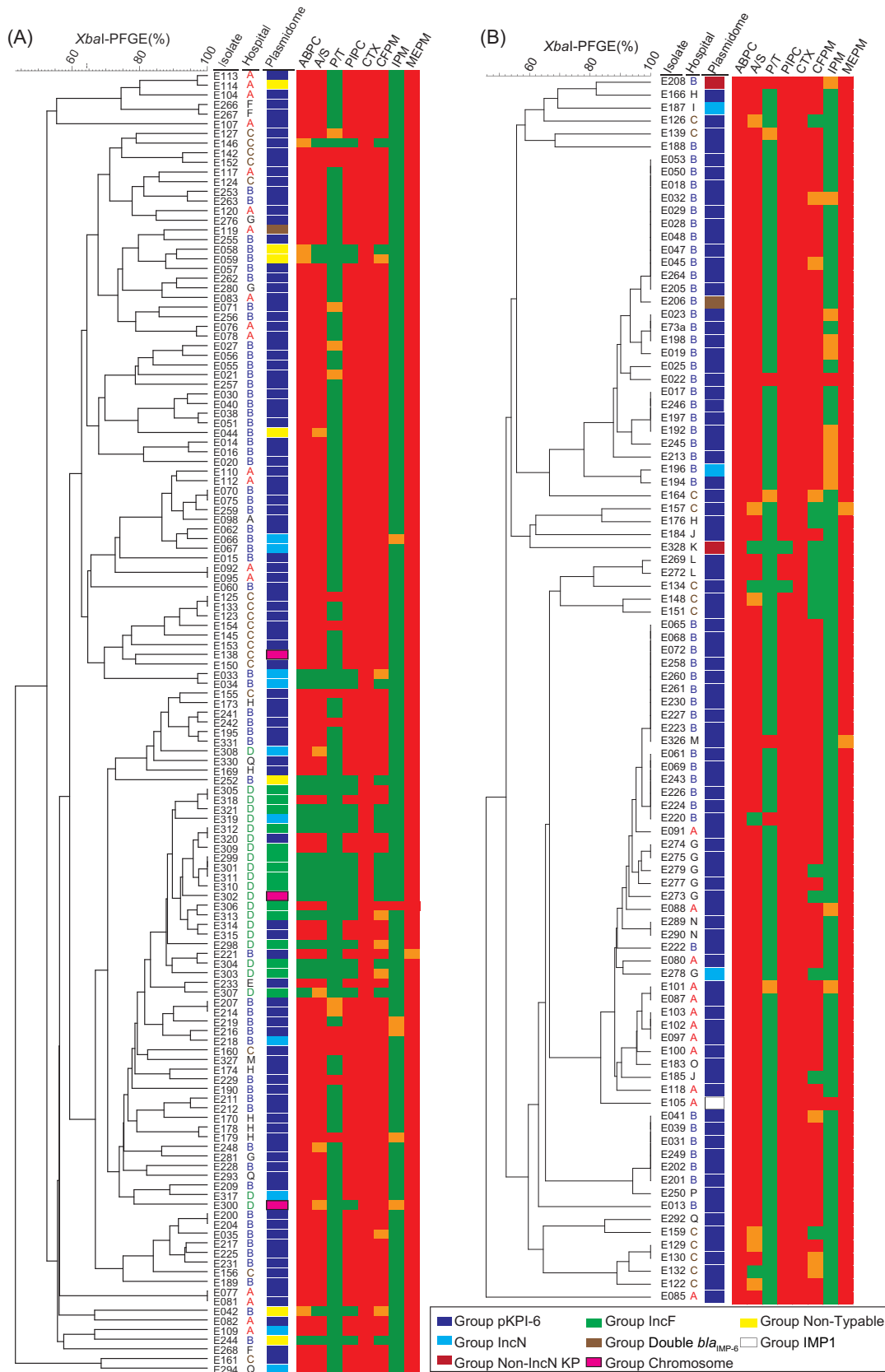


FIG 1 Phylogenetic trees based on XbaI-PFGE and classification of plasmidome carrying *bla*_{IMP} and antimicrobial resistance patterns. The plasmidome carrying *bla*_{IMP} of *E. coli* (A) and *K. pneumoniae* (B) isolates was classified according to the size and replicon type of the *bla*_{IMP}-carrier plasmids, determined by S1-PFGE and Southern blotting for *bla*_{IMP-6} and *repA* on the IncN

(Continued on next page)

mids that had integrated IncF-type plasmids framed by insertion sequences (see Fig. S2A to G and Table S1). In addition, two isolates (E208 and E328) of *K. pneumoniae* harbored plasmids categorized as group non-IncN KP (Fig. 1B). These plasmids comprised a cassette carrying *bla*_{IMP-6} without IncN-type *repA* of the pKPI-6 plasmid integrated into another plasmid (see Fig. S2H). Interestingly, *E. coli* isolate E119 and *K. pneumoniae* isolate E206 coharbored two distinct *bla*_{IMP-6}-encoding plasmids of different sizes and were categorized as group double *bla*_{IMP-6} (Fig. 1; see also Fig. S3A). Barring occasional isolations of organisms coharboring different carbapenemase genes (13, 14), few studies have shown the coexistence of two identical carbapenemase genes on different plasmids within an isolate (15). WGS revealed that isolate E119 carried pKPI-6 and an IncF-type plasmid (pEC743_1) that had a *bla*_{IMP-6} cassette from pKPI-6 integrated (49) (see Fig. S3B and C).

Characterization of IncF plasmids encoding *bla*_{IMP-6}. In addition to the *K. pneumoniae* isolates carrying group non-IncN KP plasmids, *E. coli* isolates carrying plasmids without IncN replicon were found in a single hospital (hospital D; Fig. 1A). WGS of these isolates revealed that they harbored nearly identical *bla*_{IMP-6}-encoding plasmids with an IncFIA-type replicon (categorized as group IncF) (Fig. 2A; see also Table S1). These plasmids were generated by integration of a cassette carrying *bla*_{IMP-6} on pKPI-6 into another IncF plasmid at IS26. This IncF plasmid (pEC302/04; Fig. 2B) has been reported to transmit antimicrobial resistance since 1965 (16).

The MICs of meropenem for the *E. coli* isolates carrying group IncF plasmids were low compared to those of *E. coli* isolates harboring other *bla*_{IMP-6}-encoding plasmids, such as pKPI-6 (see Fig. S4). Mutations or deletions in the porin (*OmpF*) gene in *E. coli* have been reported to enhance resistance to β -lactams (17). However, all *E. coli* isolates carrying group IncF plasmids had a premature termination codon within *ompF*, whereas the other isolates carried wild-type *ompF* (Table 1; see also Table S2). MICs of meropenem were low for these group IncF plasmid-carrying isolates, despite them being *OmpF* deficient. To investigate carbapenem resistance in the same genetic background, plasmids from representative isolates in each *bla*_{IMP-6} carriage group were transformed into the *E. coli* TOP10 strain and MICs for the transformants were determined. Transformant T305 carrying pE305_IMP6_{single} of group IncF from *E. coli* isolate E305 was more susceptible to meropenem than transformants carrying *bla*_{IMP-6}-harboring plasmids of groups (Table 2). The transcription of *bla*_{IMP-6} in the pE305_IMP6_{single} transformant was significantly lower than that in the pKPI-6 transformant (see Fig. S5A), although the plasmid copy numbers in the bacterial cells were comparable (see Fig. S5B). These results indicated that the lower MICs of meropenem in *E. coli* isolates carrying group IncF plasmids were due to the reduced transcription of *bla*_{IMP-6}.

Heteroresistance to carbapenems: enhanced resistance through gene amplification. *E. coli* isolates E305 and E318 were found to carry group IncF plasmids, and WGS revealed that their chromosomes were nearly identical (query: E318, identity 100%, coverage 100%; query: E305, identity 100%, coverage 98% [in BLASTN]). Isolate E318 harbored genes encoding extended-spectrum β -lactamases (ESBLs), such as *bla*_{CTX-M-14} and *bla*_{TEM-1B'}, on a plasmid other than pE318_IMP6, whereas isolate E305 did not have these genes (Table 3). IMP-6 confers resistance to cephalosporins and meropenem but hydrolyzes penicillins very poorly (18). Therefore, isolate E318 exhibited broader anti-

FIG 1 Legend (Continued)

plasmid. The plasmidome carrying *bla*_{IMP} was classified as follows: blue, group pKPI-6, pKPI-6-like plasmid (~50 kbp, encoding *repA* for IncN plasmid); light blue, group IncN, plasmid with *repA* for IncN, but not ~50 kbp; red, group non-IncN KP, plasmid without *repA* for IncN harbored by *K. pneumoniae*; green, group IncF, plasmid without *repA* for IncN harbored by *E. coli*; brown, group double *bla*_{IMP-6}, multiple plasmids with *bla*_{IMP-6} carried by a single isolate; enclosed pink, group chromosome, chromosomal *bla*_{IMP-6}; yellow, group non-typeable, failure to determine the size of plasmid carrying *bla*_{IMP-6}; and white, group IMP1, *bla*_{IMP-1}-carrier plasmid. Hospitals where the isolates were obtained are indicated as A to Q. Antimicrobial resistance measured by the broth microdilution method is indicated as follows: red, resistant; orange, intermediate; green, susceptible. Abbreviations: ABPC, ampicillin; A/S, ampicillin/sulbactam; P/T, piperacillin-tazobactam; PIPC, piperacillin; CTX, cefotaxime; CFPM, cefepime; IPM, imipenem; MEPM, meropenem.

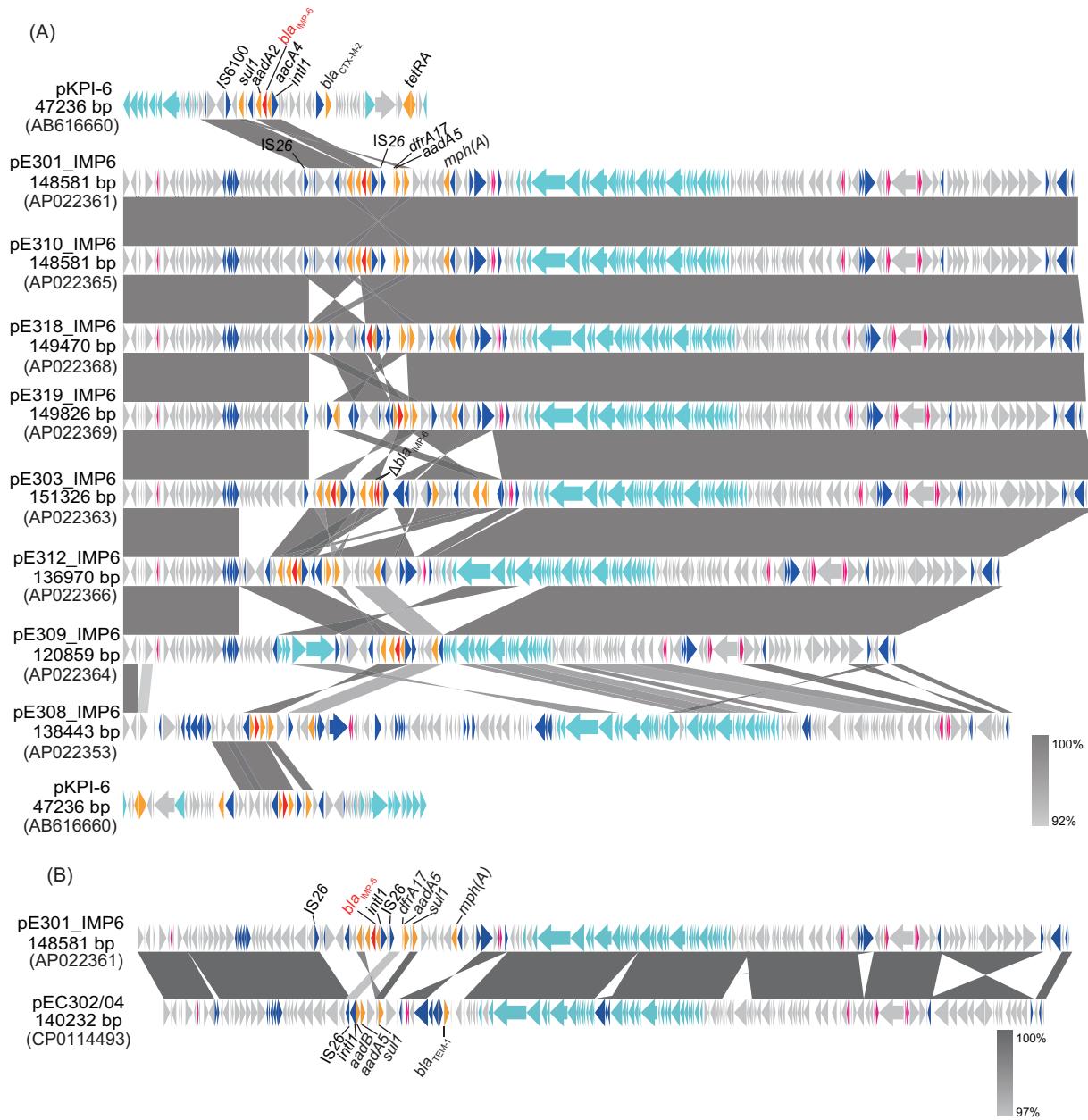


FIG 2 Comparison of plasmids in group IncF and the ancestor of these plasmids. (A) Comparison of plasmids in group IncF with plasmid pKPI-6. In addition to showing high similarity to each other, the region containing *bla_{IMP-6}* bracketed by a set of IS26 was identical to a part of pKPI-6. Block arrows indicate confirmed or putative open reading frames (ORFs), and their orientations. Arrow size is proportional to the predicted ORF length. The color code is as follows: red, carbapenem resistance gene; yellow, other antimicrobial resistance gene; light blue, conjugative transfer gene; blue, mobile element; and purple, toxin-antitoxin. Putative, hypothetical, or unknown genes are represented as gray arrows. The gray-shaded area indicates regions with high identity between the two sequences. Accession numbers of the plasmids are indicated in brackets. (B) Ancestor of plasmid pE301_IMP6. The backbone of plasmid pE301_IMP6 which is representative of the plasmids in group IncF, corresponded to the structure of plasmid pEC302_04 reported in Malaysia in 2004.

microbial resistance than isolate E305. In contrast, the MIC of meropenem for E305 was higher than that for E318.

WGS of E305 and E318 revealed the complete sequence of pE318_IMP6; however, it failed to determine the complete sequence of pE305_IMP6. Therefore, to analyze the structure of pE305_IMP6, we used a combination of WGS, Southern blotting, and qPCR analysis. The length and depth of each contig of pE305_IMP6 deduced from WGS are shown in the *de novo* assembly graphs generated using the Bandage software (19) in Fig. 3A. The total length of pE305_IMP6 deduced from WGS data were ~149 kbp.

TABLE 1 Numbers of isolates carrying a porin gene with mutation(s)^a

Strain	Group	No. of isolates carrying mutation(s)			Total no. of sequenced isolates
		<i>ompC</i> <i>ompK35</i>	<i>ompF</i> <i>ompK36</i>	<i>ompC+ompF</i> <i>ompK35+ompK36</i>	
<i>E. coli</i>	pKPI-6	0	2	0	14
	IncN	1	2	1	9
	IncF	0	11	0	11
	Double <i>bla</i> _{IMP}	0	0	0	1
	Chromosome	0	2	0	3
<i>K. pneumoniae</i>	pKPI-6	1	7	0	29
	IncN	0	1	0	2
	Non-IncN KP	0	0	0	2

^aGroups correspond to those in Fig. 1. *E. coli* and *K. pneumoniae* isolates were sequenced using Illumina HiSeq 3000 or Illumina MiSeq, and the sequences were compared to the following reference sequences: *ompC* and *ompF* sequences for *E. coli* strain MG1655 (K-12 substrain) and *ompK35* and *ompK36* sequences for *K. pneumoniae* strain ATCC 13883. Mutant porin was defined as having <90% identity or <90% coverage.

However, according to Southern blotting results, pE318_IMP6 and pE305_IMP6 were ~145 and ~200 kbp in size, respectively (Fig. 3B). Based on the depth of each contig, the copy number of each contig was predicted as follows: Contig3, 1 copy; Contig2 and Contig5, 6 copies; Contig1 and Contig6, 3 copies; and Contig4, 5 copies (Fig. 3A). Therefore, pE305_IMP6 was predicted to have an ~19-kbp repeat region consisting of triplication of Contig1 and Contig6, sextuplication of Contig2 and Contig5, and quintuplication of Contig4 (Fig. 3C). Except for the repeat region, pE305_IMP6 and pE318_IMP6 exhibited high sequence similarity (identity, 99.27%; coverage, 100%) (Fig. 3D). The *bla*_{IMP-6} gene was located on Contig6 and was predicted to be triplicated. qPCR analysis corroborated that pE305_IMP6 carried three copies of *bla*_{IMP-6}, whereas pE318_IMP6 harbored a single copy (see Fig. S5C). *bla*_{IMP-6} transcription was significantly higher in isolate E305 than in isolate E318 (Fig. 3E), even though the *bla*_{IMP-6}-carrier plasmid copy numbers in the cells of these isolates were not significantly different (see Fig. S5D). Triplication of *bla*_{IMP-6} in tandem resulted in a higher transcription level in E305 and thus a higher level of resistance to meropenem.

Subculture of the clonal isolate E305 in broth medium revealed a mixture of subpopulations of bacteria carrying a plasmid with multiple *bla*_{IMP-6} copies (which represented the majority) and bacteria carrying a plasmid with a single *bla*_{IMP-6} copy. In Southern blotting analyses for *bla*_{IMP-6}, a faint band at ~145 kbp was observed in addition to the major band at ~200 kbp (Fig. 3B). It was also found that T305 (a

TABLE 2 MICs of meropenem and conjugation efficiency in transformants with plasmids from representative isolates in each group^a

Original species	Group	Original host isolate	MIC (mg/liter)	Avg conjugation efficiency ± SD
<i>E. coli</i>	pKPI-6	E174	4	$(8.1 \pm 3.8) \times 10^{-2}$
	IncN	E066	16	$(2.2 \pm 3.1) \times 10^{-4}$
	IncN	E033	16	$(2.4 \pm 1.3) \times 10^{-2}$
	IncF	E305	<1	$(7.5 \pm 2.3) \times 10^{-4}$
<i>K. pneumoniae</i>	pKPI-6	E188	4	$(3.7 \pm 2.0) \times 10^{-1}$
	IncN	E187	4	$(2.9 \pm 1.1) \times 10^{-1}$
	IncN	E196	16	$(4.4 \pm 3.5) \times 10^{-1}$
	Non-IncN KP	E208	4	0
	Non-IncN KP	E328	2	$(3.1 \pm 2.6) \times 10^{-4}$

^aGroups correspond to those in Fig. 1. Plasmids from representative isolates in each group were transformed into *E. coli* TOP10 strain by electroporation. MICs of meropenem for these transformants were measured by the broth microdilution method, in triplicate. The conjugation assay was conducted by mating the transformants as donors and *E. coli* TUM3456 as a recipient. The conjugation frequency was calculated as the CFU number of transconjugants per number of donors plus transconjugants. Average conjugation efficiencies from triplicate assays are indicated.

TABLE 3 Comparison of *E. coli* isolates E305 and E318^a

<i>E. coli</i> isolate	Group	Antimicrobial MIC (mg/liter)								Porin		Meropenem MIC (mg/liter)		ESBL	
		ABPC	A/S	P/T	PIPC	CTX	CFPM	IPM	MEPM	OmpC	OmpF	Etest	BMD	Plasmid	Others
E305	IncF	≤8 (S)	≤8/4 (S)	≤16 (S)	≤8 (S)	>2 (R)	>16 (R)	≤1 (S)	>2 (R)	W/T	PSC	>32	16	(-)	(-)
E318	IncF	>16 (R)	>16/8 (R)	≤16 (S)	>64 (R)	>2 (R)	>16 (R)	≤1 (S)	>2 (R)	W/T	PSC	4	8	(-)	<i>bla</i> _{CTX-M-14} <i>bla</i> _{TEM-1B}

^aGroups correspond to those presented in Fig. 1. ABPC, ampicillin; A/S, ampicillin/sulbactam; P/T, piperacillin-tazobactam; PIPC, piperacillin; CTX, cefotaxime; CFPM, cefepime; IPM, imipenem; MEPM, meropenem. R or S in parentheses indicates resistance or susceptibility, respectively, based on CLSI M200-S26. W/T, wild type; PSC, premature stop codon. Meropenem MICs were measured using either the Etest or broth microdilution (BMD). ESBL genes encoded on *bla*_{IMP-6}-carrier plasmid (Plasmid) and on others (Others) are indicated in the last two columns.

transformant of pE305_IMP6_{single} extracted from E305) carried an ~145-kbp plasmid without *bla*_{IMP-6} amplification due to *recA* deficiency in the recipient *E. coli* TOP10 strain (see Fig. S5E) (20). qPCR analysis confirmed that T305 carried one *bla*_{IMP-6} copy on its plasmid (see Fig. S5F). These results indicated the existence of a subpopulation carrying

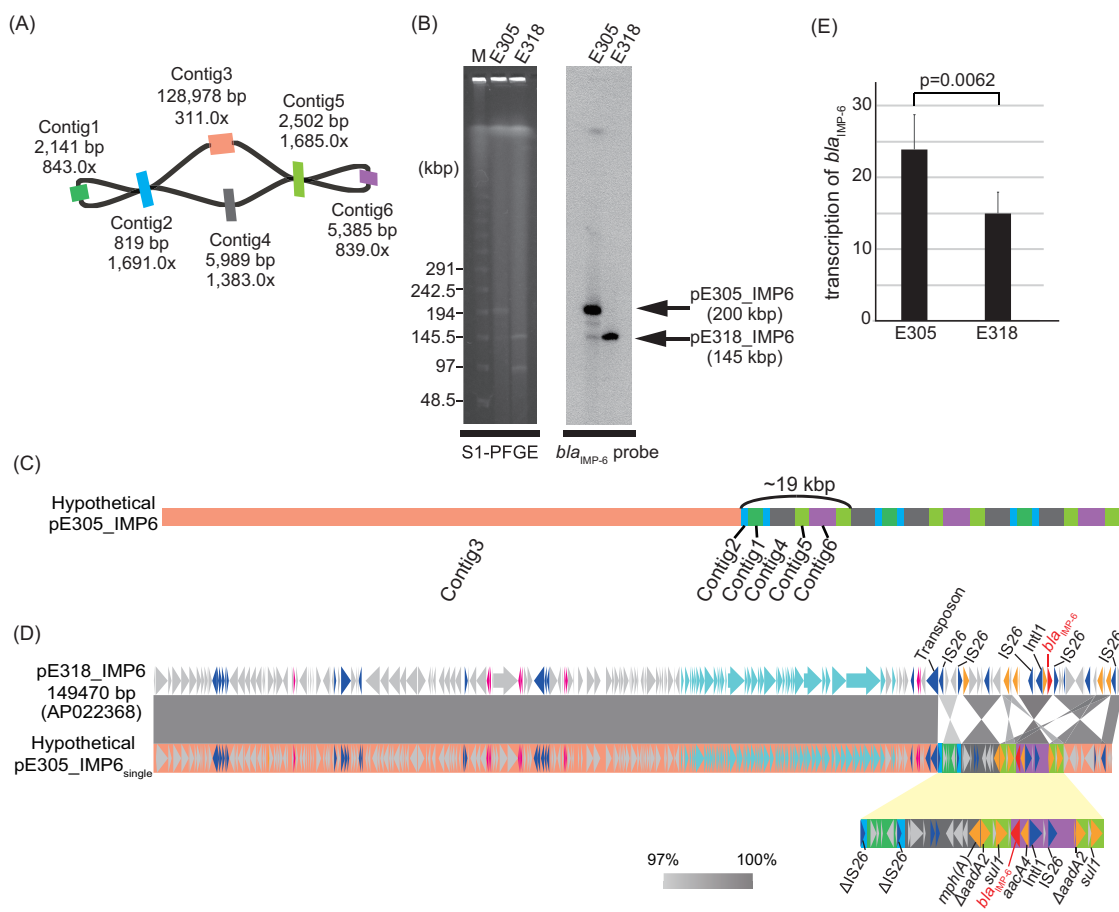


FIG 3 Genomic structure of group IncF plasmid pE305_IMP6 and enhanced transcription of *bla*_{IMP-6}. (A) Genomic structure of plasmid pE305_IMP6. *De novo* assembly graph of plasmid pE305_IMP6 visualized by Bandage displays the connections between contigs. The length and depth of each contig are shown. Contig2 connects Contig1 with Contig3 or Contig4, and Contig5 connects Contig6 with Contig3 or Contig4. (B) Sizes of plasmids pE305_IMP6 and pE318_IMP6. PFGE of S1-digested genomic DNA from *E. coli* isolates E305 and E318, followed by Southern blotting with a *bla*_{IMP-6} probe, indicated the size of each plasmid. M, DNA size marker (lambda ladder; Bio-Rad). (C) Hypothetical structure of pE305_IMP6. The colors correspond to the colors of contigs in panel A. (D) Genomic comparison of pE318_IMP6 and hypothetical pE305_IMP6_{single}. According to the overlap between contigs of pE305_IMP6, the hypothetical sequence shown was assembled and compared to the sequence of plasmid pE318_IMP6. Except for the repeats, pE305_IMP6_{single} and pE318_IMP6 were highly similar. Block arrows indicate confirmed or putative ORFs and their orientations. The color code, arrows, and similarity are as described in the legend of Fig. 2. The colors under arrows of pE305_IMP6_{single} correspond to the colors of contigs in panel A. (E) Transcript levels of *bla*_{IMP-6} in *E. coli* isolates E305 and E318. qPCR revealed significantly higher transcription of *bla*_{IMP-6} in isolate E305 than in isolate E318. The bar chart represents the mRNA transcript ratio of *bla*_{IMP-6} to the housekeeping gene *rrsA*, which was used as a reference gene. Bars indicate means ± standard deviations, calculated from sextuplet experiments. The *P* value was calculated by using the Mann-Whitney U test.

a plasmid with one *bla*_{IMP-6} copy within *E. coli* isolate E305, whereas the majority of the population carried a plasmid harboring three copies of *bla*_{IMP-6}.

Comparison of CRE isolates carrying pKPI-6 with those carrying other groups of plasmids harboring *bla*_{IMP-6}. *bla*_{CTX-M-2}, which is an ESBL gene located distant from *bla*_{IMP-6} on pKPI-6, compensated for the narrow range of hydrolysis of β -lactams by IMP-6 (11, 18). However, these two β -lactamase genes were not always transferred together from pKPI-6 to another plasmid. Plasmids categorized as group non-IncN KP and group IncF did not carry ESBL genes (see Table S3) and rarely conferred resistance to penicillins, in contrast to pKPI-6, which confers broad resistance to β -lactams (Fig. 1). We next measured the conjugation efficiency of representative plasmids in each group (Table 2). pKPI-6 plasmids and group IncN plasmids, which had the entire pKPI-6 plasmid incorporated, showed a higher conjugation efficiency than group non-IncN KP/IncF plasmids. These characteristics may have facilitated the vast horizontal dissemination of pKPI-6 in the study area.

Compared with the chromosomal diversity among *E. coli* isolates bearing pKPI-6, *K. pneumoniae* isolates carrying pKPI-6 exhibited higher clonality as indicated by pulsed-field gel electrophoresis with XbaI (XbaI-PFGE) analysis (Fig. 1). This may be explained by the presence of the *kikA* gene on pKPI-6, the product of which reportedly promotes cell death of *K. pneumoniae* following conjugation (21). The conjugation efficiency of pKPI-6 into *K. pneumoniae* ATCC 13883 was considerably lower than that into *E. coli* TUM3456 (3.3×10^{-4} and 3.7×10^{-1} , respectively). Maybe only “*kikA*-resistant” *K. pneumoniae* are able to acquire pKPI-6, leading to clonal similarity among the *K. pneumoniae* isolates bearing pKPI-6.

Chromosomal integration of *bla*_{IMP-6}. Unlike most CRE isolates, which carried the predominant pKPI-6 or other *bla*_{IMP-6}-encoding plasmids, 3 of 135 *E. coli* isolates (E138, E300, and E302) harbored *bla*_{IMP-6} on their chromosomes, as indicated by S1-PFGE followed by Southern blotting with *bla*_{IMP-6} probes (Fig. 1A and Fig. 4A). I-Ceul-PFGE followed by Southern blotting with probes for the *bla*_{IMP-6} and 16S rRNA genes confirmed chromosomally located *bla*_{IMP-6} (Fig. 4B). WGS revealed that the chromosome of isolate E138 had a cassette harboring *bla*_{IMP-6} integrated, framed by a set of IS15 (Fig. 4C). The chromosomes of E300 and E302 had IncFIA plasmids carrying *bla*_{IMP-6} integrated (Fig. 4D and E). Although these plasmids were essentially identical to pE301_IMP6 (*E. coli*, group IncF), these isolates were phylogenetically distinct on the XbaI-PFGE phylogenetic tree (Fig. 1).

Emergence of pKPI-6-like plasmid harboring *bla*_{IMP-1}. One *K. pneumoniae* isolate, E105, harbored *bla*_{IMP-1}, which is a single-nucleotide variant of *bla*_{IMP-6}, within a clonal cluster of pKPI-6 carriers (Fig. 1B). Due to this mutation, E105 was resistant to imipenem, whereas most isolates carrying *bla*_{IMP-6} were susceptible to this antibiotic. WGS revealed that plasmids pKPI-6, pE013_IMP6 (plasmid group pKPI-6), and pE105_IMP1 were 99.8% identical, with a coverage of 100% (query: pE013_IMP6) (Fig. 5). The only difference was the presence of a 714-bp region bracketed by a set of homologous regions in pE013_IMP6.

DISCUSSION

IMP-producing *Enterobacteriaceae* have been reported sporadically on a global basis (2). IMP-4-producing *Enterobacteriaceae* are endemic to Australia (22), and IMP-1, -4, and -8 producers have been occasionally detected in China (23). Our study revealed the exclusive dissemination of IMP-6 producers (95% of CRE isolates) in northern Osaka, Japan, consistent with findings in previous studies (11, 24, 25). By analyzing the plasmidome transmitting *bla*_{IMP}, we clarified the relationships between *bla*_{IMP}-harboring isolates that seemed diverse based on XbaI-PFGE analysis or comparison of short-read WGS results.

The present study revealed predominant dissemination of pKPI-6 in the study area, which may have resulted in the emergence of diverse derivatives. Group IncF plasmids possessed similar genomic structures, consisting of the globally disseminated IncF plasmid and a *bla*_{IMP-6} cassette cointegrated on the pKPI-6 genome, without accompaniment of *bla*_{CTX-M-2} (Fig. 2). Our analysis revealed that *bla*_{IMP-6} transcription was

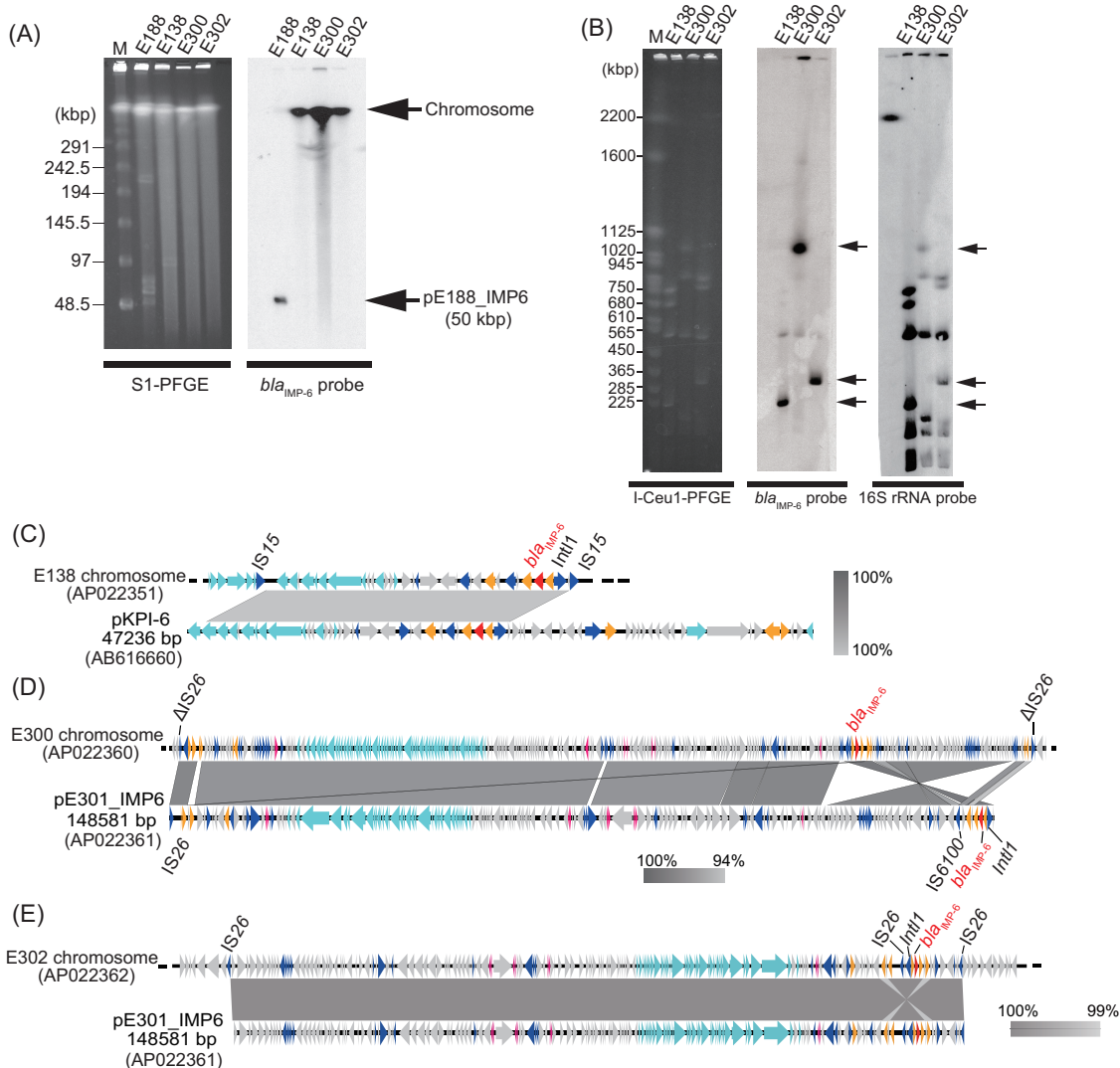


FIG 4 Chromosomal integration of *bla*_{IMP-6}. (A) S1-PFGE followed by Southern blotting with a *bla*_{IMP-6} probe. Arrows indicate the segments carrying *bla*_{IMP-6} in *E. coli* isolates E138, E300, and E302 (group chromosome) and *K. pneumoniae* isolate E188 (group pKPI-6). M, DNA size marker (lambda ladder; Bio-Rad). (B) I-Ceu1-PFGE followed by Southern blotting with *bla*_{IMP-6} and 16S rRNA probes. Arrows indicate the segments encoding *bla*_{IMP-6} or 16S rRNA, proving that *bla*_{IMP-6} and 16S rRNA were located on the same segment. M, DNA size marker (*Saccharomyces cerevisiae* ladder; Bio-Rad). (C) Chromosomal integration of a region carrying *bla*_{IMP-6} in isolate E138. A 23-kbp region containing *bla*_{IMP-6} of plasmid pKPI-6 was integrated in the chromosome of isolate E138. This region was bracketed by a set of IS15. (D) Comparison of the chromosomal genomic structure of isolate E300 with plasmid pE301_IMP6. Isolate E300 carried chromosomal *bla*_{IMP-6}, and the region bracketed by a set of mutated IS26 showed high similarity with plasmid pE301_IMP6 in group IncF. (E) Chromosomal integration of plasmid pE301_IMP6 in isolate E302. Isolate E302 acquired chromosomal *bla*_{IMP-6} by incorporation of plasmid pE301_IMP6 bracketed by a set of IS26. The color code is the same as that described in the legend of Fig. 2.

lower from group IncF plasmid (pE305_IMP6_{single}) than from pKPI-6 in *E. coli* cells of the same genetic background (see Fig. S5A). Low carbapenemase gene transcription is considered one of the reasons for reduced resistance to meropenem (26). Therefore, CRE isolates carrying group IncF plasmids might have a reduced fitness cost for the carriage of *bla*_{IMP-6}, leading to further environmental dissemination of *bla*_{IMP-6} (27).

Unlike for other plasmids in group IncF, the complete sequence of pE305_IMP6 could not be obtained by long-read or short-read sequencing because of a signature 19-kbp repeat sequence unit. Based on combined WGS, Southern blotting, and qPCR data, we proposed a hypothetical structure of pE305_IMP-6 (Fig. 3C). Our results indicated that, despite its clonal origin, CRE isolate E305 comprised two different populations: a major population carrying pE305_IMP-6 with multiple *bla*_{IMP-6} copies

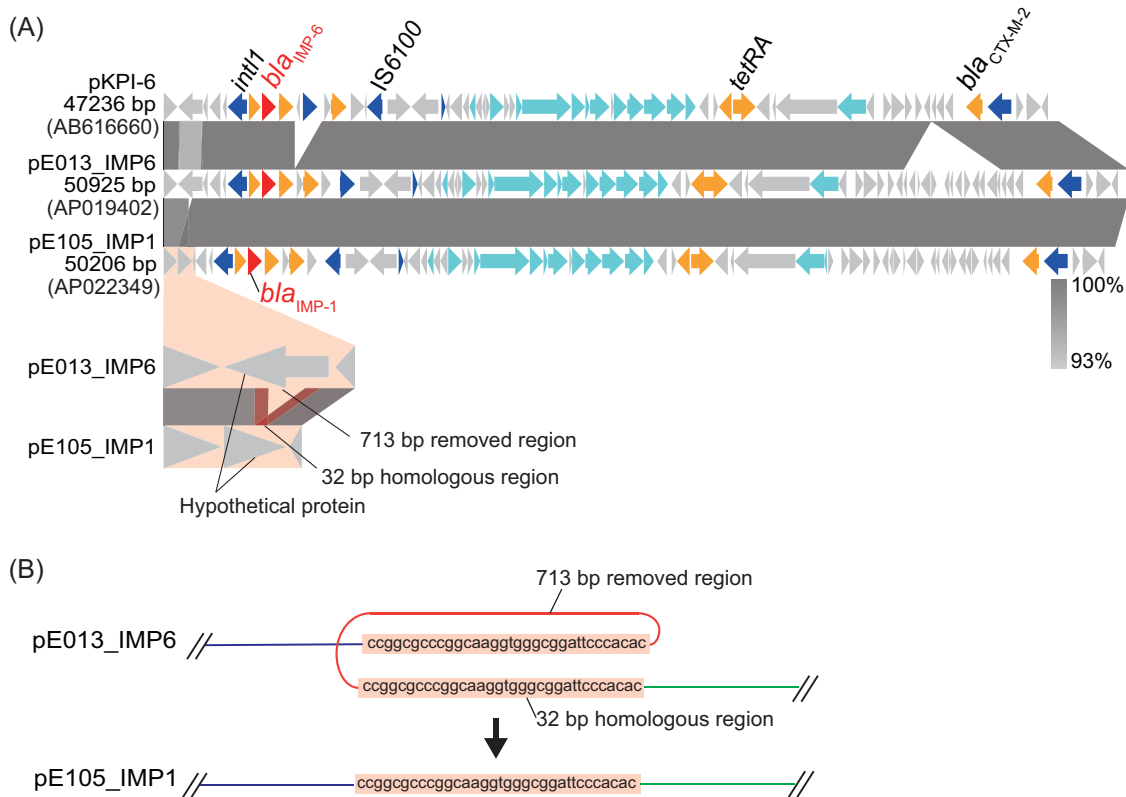


FIG 5 Plasmid pE105_IMP1 carrying *bla_{IMP-1}* was derived from plasmid pKPI-6 by homologous recombination. (A) Comparison of the pE105_IMP1 and pKPI-6 plasmids. The genomic structure of pE105_IMP1 (group IMP1) was compared to plasmids pKPI-6 and pE013_IMP6 (group pKPI-6) obtained from *K. pneumoniae* isolate E013. Differences between pE105_IMP1 and pE013_IMP6 are visually extended at the bottom. The color code is the same as that described in the legend of Fig. 2. (B) Schematic chart of homologous recombination. The 713-bp region of plasmid pE013_IMP6 was removed by homologous recombination at the 32-bp region.

and a minor population carrying pE305_IMP-6_{single} with a single *bla_{IMP-6}* copy (Fig. 3B; see also Fig. S5E and F). Moreover, the amplification of *bla_{IMP-6}* on the IncF plasmid enhanced the transcription of *bla_{IMP-6}* (Fig. 3E), resulting in increased resistance to meropenem (Table 3). These results are consistent with previous studies reporting higher resistance to carbapenem through amplification of *bla_{OXA-58}* (28) and *bla_{NDM-1}* (20).

All *E. coli* isolates carrying group IncF plasmids were found to possess *ompF* with a premature termination codon (see Table S2). When an isolate producing wild-type OmpF carries this plasmid with a single copy of *bla_{IMP-6}*, the isolate is difficult to detect due to weaker resistance to meropenem. However, when an isolate with a porin mutation acquires a group IncF plasmid with multiple *bla_{IMP-6}* copies, it may abruptly exhibit strong resistance to meropenem without any direct trace of horizontal transfer. These types of plasmids may act as “hidden transmitters” of *bla_{IMP-6}*.

Moreover, we demonstrated chromosomal integration of group IncF plasmids in some *E. coli* isolates. Carbapenemase genes have been reported to be transmitted primarily through plasmid conjugation (4), and chromosomal integration has been reported in a limited number of strains (29). In our study, 3 of 135 *E. coli* isolates (2.2%) exhibited chromosomal integration of *bla_{IMP-6}*, which presumably occurred during the vast horizontal spread of pKPI-6. Compared to *bla_{IMP-6}* on plasmids, chromosomal *bla_{IMP-6}* was not readily transmissible to another patient. However, these isolates may stably possess *bla_{IMP-6}* within a patient and not lose carbapenem resistance through the elimination of plasmids harboring *bla_{IMP-6}*.

In the early 1990s, some unique metallo- β -lactamases were reported in Japan (30, 31), followed by the identification of IMP-1 (32). Since then, these β -lactamases have

been frequently identified in Japan (33). The single amino acid variant, IMP-6, was identified in 2001 (18). IMP-1 producers have disseminated mainly in eastern Japan, including Tokyo (24, 34), whereas IMP-6 producers have been almost exclusively found in western Japan, including Osaka (7, 10, 11, 25). Consistent with these findings, in the present study only one *K. pneumoniae* isolate carrying bla_{IMP-1} , E105, was isolated in hospital A, where CRE carrying pKPI-6 were dominant. The patient carrying CRE isolate E105 was hospitalized for 512 days with other inpatients carrying CRE with pKPI-6, and the isolate showed ~83% similarity with a cluster of *K. pneumoniae* isolates carrying pKPI-6 in the XbaI-PFGE phylogeny (Fig. 1B). In addition, WGS of the plasmids revealed that a 714-bp region bracketed by 32-bp homologous regions was the only difference between pE105_IMP1 and pE013_IMP6 (Fig. 5A). This very small fragment appeared to have been removed by homologous recombination in pE105_IMP1 (Fig. 5B). Our results suggest that bla_{IMP-6} had disseminated via the transmission of pKPI-6, and spontaneous mutation may have generated the bla_{IMP-1} -encoding plasmid providing broader antimicrobial resistance, resulting in increased fitness in the clinical setting.

This multi-institutional surveillance study uncovered the clonal dissemination of a plasmid encoding a specific carbapenemase IMP-6 and demonstrated that a seemingly clonal horizontal dissemination of CRE isolates had embraced heterogeneous minor subpopulations, which exhibited broadened antimicrobial resistance, stable carriage of bla_{IMP-6} through chromosomal integration, or heteroresistance related to covert bla_{IMP} transmission. Such diverse gene adaptations might also be common among CRE isolates carrying other carbapenemase genes. By multifaceted analysis of the plasmidome, this study revealed the vast regional dissemination of a carbapenemase-encoding plasmid, along with the presence of diverse derivatives that would ensure and facilitate the dissemination of carbapenemase genes in various environments, resulting in serious complications in clinical settings.

MATERIALS AND METHODS

CRE isolates and PFGE phylogenetic analysis. We performed a CRE surveillance study of 1,507 patients hospitalized in 43 hospitals located in northern Osaka between December 2015 and January 2016 (10). In the present study, we analyzed 230 CRE isolates carrying bla_{IMP} obtained in the surveillance study, including 135 *E. coli* isolates and 95 *K. pneumoniae* isolates. All isolates were subjected to XbaI-digested PFGE for phylogenetic analysis (35). Dendrograms were generated from PFGE patterns by the UPGMA method using BioNumerics software (version 6.6; Applied Maths NV, Sint-Martens-Latem, Belgium).

Classification of bla_{IMP} carriage by PFGE and Southern blotting. The size and replicon type of bla_{IMP} -harboring plasmids were determined by S1-nuclease-digested PFGE followed by Southern hybridization (S1 nuclease was obtained from TaKaRa Bio, Shiga, Japan). S1-PFGE and Southern blot hybridization for the bla_{IMP-6} and *repA* genes encoded on the IncN-type plasmid were performed as described in our previous study (12). The sizes of bla_{IMP} -encoding plasmids were determined using BioNumerics software (version 7.5; Applied Maths NV). The modes of bla_{IMP} carriage were classified into seven groups based on the sizes and replicon types of the plasmids carrying bla_{IMP} . The groups and their associated characteristics are as follows: group pKPI-6, a pKPI-6-like bla_{IMP-6} -encoding plasmid (~50 kbp, encoding *repA* for IncN plasmid); group IncN, a bla_{IMP-6} -encoding plasmid (not ~50 kbp, encoding *repA* for IncN plasmid); group non-IncN KP, a bla_{IMP-6} -encoding plasmid (without *repA* for IncN plasmid) harbored by *K. pneumoniae* isolates; group IncF, a bla_{IMP-6} -encoding plasmid (without *repA* for IncN plasmid) harbored by *E. coli* isolates; group double bla_{IMP-6} , multiple plasmids with bla_{IMP-6} harbored by a single isolate; group chromosome, chromosomal bla_{IMP-6} ; group non-typeable, a bla_{IMP-6} -encoding plasmid of unknown size; group IMP1, a bla_{IMP-1} -carrier plasmid.

Isolates classified as chromosomal bla_{IMP} carriers were further analyzed to identify the location of bla_{IMP} . In brief, I-CeuI endonuclease-digested PFGE followed by Southern blotting using probes for bla_{IMP-6} and 16S rRNA genes was performed to confirm the location of the bla_{IMP} gene in three *E. coli* isolates—E138, E300, and E302—as previously described (29).

Antimicrobial susceptibility testing. Susceptibility to ampicillin, ampicillin/sulbactam, piperacillin-tazobactam, piperacillin, cefotaxime, cefepime, imipenem, and meropenem was determined by the broth microdilution method according to the Clinical and Laboratory Standards Institute document M100-S28 (36). MICs of meropenem were determined using Etest (bioMérieux, Marcy l'Etoile, France), following the manufacturer's instructions. *E. coli* ATCC 25922 was used as a control strain.

Whole-genome sequencing and genomic analysis. Genomic DNA for long- and short-read sequencing was extracted by using a DNeasy PowerSoil kit (Qiagen, Hilden, Germany). Short-read sequencing was conducted on an Illumina HiSeq 3000 sequencer using the KAPA library preparation kit (Kapa Biosystems, Woburn, MA) or on an Illumina MiSeq sequencer using the KAPA HyperPlus Library Preparation kit (Kapa Biosystems). Long-read sequencing was conducted on a Nanopore GridION

sequencer (Oxford Nanopore Technologies, Oxford, UK) using sn SQK-LSK109 1D ligation sequencing kit and sn EXP-NBD103 native barcoding kit. The reads were assembled and polished using Unicycler (37). In cases where the complete plasmid sequences could not be constructed, sequences were assembled with CANU (version 1.8) (38) or flye (39) and improved using Pilon (40) or Racon (41). The PlasmidFinder (42) and ResFinder (43) databases were used to identify antimicrobial resistance genes and plasmid replicon types, respectively. A detailed analysis of the insertion sequence was performed using ISfinder (44). The sequences were annotated with RASTtk (45), and the genomic structures were compared with EasyFig (46). Plasmids similar to those found in this study were identified using BLAST.

Transformation and bacterial transconjugation assay. Plasmids were prepared from overnight cultures of *E. coli* isolates E033, E066, E174, and E305 and *K. pneumoniae* isolates E187, E188, E196, E208, and E328, using a plasmid miniprep kit (Qiagen). Electrocompetent TOP10 *E. coli* cells (Invitrogen, Waltham, MA) were electroporated with the extracted plasmids using a Gene Pulser Xcell system (Bio-Rad, Hercules, CA). After incubation in S.O.C. medium (Invitrogen) for 2 h (6 h for isolate E305), transformants were selected on Luria-Bertani (LB) agar supplemented with 0.125 $\mu\text{g/ml}$ meropenem (2 $\mu\text{g/ml}$ cefotaxime for isolate E305).

Bacterial conjugation assays were performed using the transformants as donors and the sodium azide-resistant *E. coli* strain TUM3456 (47) as a recipient. After mixing overnight cultures of donors and recipients at a 1:10 volumetric ratio, the mixture (10 μl) was incubated on LB agar for 24 h at 37°C. Transconjugants were selected on LB agar containing cefotaxime (2 $\mu\text{g/ml}$) and sodium azide (150 $\mu\text{g/ml}$). The conjugation frequency was calculated from the CFU as the number of transconjugants divided by the number of donors plus transconjugants.

Determination of the plasmid copy number per host bacterial cell. DNA of *E. coli* isolates E305 and E318, and *E. coli* transformants with plasmids pE188_IMP6 and pE305_IMP6_{single} (T188 and T305, respectively) was extracted using the DNA minikit (Qiagen). Using qPCR, the copy numbers of the *repA2* gene on plasmids pE305_IMP6 and pE318_IMP6 and the *bla*_{IMP-6} gene on pE188_IMP6 were compared to the copy number of the *rrsA* gene encoding 16S rRNA on the chromosome. qPCRs were carried out using Thunderbird SYBR qPCR Mix (Toyobo Life Science, Osaka, Japan) on a LightCycler 96 system (Roche Life Science, Penzberg, Germany). Primers used for this assay are listed in Table S4 in the supplemental material. qPCR analysis was performed using data from repeated experiments ($n = 6$), and the plasmid copy number per cell was calculated from cycle threshold (C_T) values using the comparative C_T method (48).

Determination of the copy number of *bla*_{IMP-6} per plasmid. Plasmids of *E. coli* isolates E305 and E318 were extracted using a plasmid miniprep kit (Qiagen). Using qPCR, the copy numbers of the *bla*_{IMP-6} gene were compared to those of the *repA2* gene on plasmids pE305_IMP6 and pE318_IMP6. qPCRs were carried out using Thunderbird SYBR qPCR Mix on a LightCycler 96 System. Primers used for this assay are listed in Table S4. qPCR analysis was performed using data from repeated experiments ($n = 5$), and the *bla*_{IMP-6} copy number per plasmid was calculated from C_T values using the comparative C_T method.

Transcription of *bla*_{IMP-6}. *E. coli* isolates E305 and E318, and *E. coli* transformants T188 and T305 were incubated in LB broth until the optical density at 600 nm reached 0.3 to 0.4. The total RNA was extracted using the RNeasy minikit (Qiagen). RNA was treated with ReverTra Ace qPCR RT Master Mix with gDNA remover (Toyobo Life Science) to remove contaminating DNA and to reverse transcribe the RNA into cDNA. For quality control, DNase-treated RNA that had not been reverse transcribed was subjected to a DNA contamination test by qPCR. The *rrsA* gene encoding 16S rRNA served as an endogenous control for normalization. qPCRs were carried out using Thunderbird SYBR qPCR Mix on a LightCycler 96 system. Primers used for this assay are listed in Table S4. qPCR analysis was performed using data from repeated experiments ($n = 7$), and transcript levels were calculated from C_T values using the comparative C_T method.

Data availability. The WGS data are available from the DDBJ (DNA Data Bank of Japan) database under accession numbers [AB616660](#), [AP019402](#), [AP019405](#), and [AP022349](#) to [AP022369](#). Raw data of isolate E305 are available at NCBI under accession numbers [DRX184368](#) and [DRX182679](#).

SUPPLEMENTAL MATERIAL

Supplemental material is available online only.

FIG S1, EPS file, 2.6 MB.

FIG S2, EPS file, 2.6 MB.

FIG S3, EPS file, 2.5 MB.

FIG S4, PDF file, 0.6 MB.

FIG S5, EPS file, 2.8 MB.

TABLE S1, PDF file, 0.3 MB.

TABLE S2, PDF file, 0.7 MB.

TABLE S3, PDF file, 0.5 MB.

TABLE S4, PDF file, 0.3 MB.

ACKNOWLEDGMENTS

We thank Isao Nishi and Akiko Ueda, Osaka University Hospital, for assistance with antimicrobial resistance assays, and we thank Yoshikazu Ishii, Toho University Graduate School of Medicine, for providing *E. coli* TUM3456.

This study was supported by the Japan Initiative for Global Research Network on Infectious Diseases (J-GRID) from the Ministry of Education, Culture, Sport, Science and Technology in Japan and by the Japan Agency for Medical Research and Development (AMED; grants 19fm0108003h0005 and 20wm0225013h0001).

R.A. and Y.A. conceptualized study design. R.A. and R.K. performed experiments. R.A., Y.A., Y.S., D.T., Y.M., and D.M. analyzed data. R.A., Y.A., N.Y., K.T., Y.F., and S.H. drafted and revised the manuscript. All authors edited and approved of the final manuscript.

We declare that we have no competing interests.

REFERENCES

- World Health Organization. 2014. Antimicrobial resistance: global report on surveillance. World Health Organization, Geneva, Switzerland. <https://apps.who.int/iris/handle/10665/112642>. Accessed 21 May 2020.
- Logan LK, Weinstein RA. 2017. The epidemiology of carbapenem-resistant *Enterobacteriaceae*: the impact and evolution of a global menace. *J Infect Dis* 215:S28–S36. <https://doi.org/10.1093/infdis/jiw282>.
- Nordmann P, Naas T, Poirel L. 2011. Global spread of carbapenemase-producing *Enterobacteriaceae*. *Emerg Infect Dis* 17:1791–1798. <https://doi.org/10.3201/eid1710.110655>.
- Kopotsa K, Osei Sekyere J, Mbelle NM. 2019. Plasmid evolution in carbapenemase-producing *Enterobacteriaceae*: a review. *Ann N Y Acad Sci* 1457:61–91. <https://doi.org/10.1111/nyas.14223>.
- Kanamori H, Parobek CM, Juliano JJ, van Duin D, Cairns BA, Weber DJ, Rutala WA. 2017. A prolonged outbreak of KPC-3-producing *Enterobacter cloacae* and *Klebsiella pneumoniae* driven by multiple mechanisms of resistance transmission at a large academic burn center. *Antimicrob Agents Chemother* 61:e01516–16. <https://doi.org/10.1128/AAC.01516-16>.
- de Man TJB, Yaffee AQ, Zhu W, Batra D, Alyanak E, Rowe LA, McAllister G, Moulton-Meissner H, Boyd S, Flinchum A, Slayton RB, Hancock S, Spalding WM, Laufer HA, Rasheed JK, Noble-Wang J, Kallen AJ, Limbago BM. 2020. Multispecies outbreak of Verona integron-encoded metallo- β -lactamase-producing multidrug-resistant bacteria driven by a promiscuous incompatibility group A/C2. *Clin Infect Dis* <https://academic.oup.com/cid/advance-article-abstract/doi/10.1093/cid/ciaa049/5817041>. Accessed 22 May 2020.
- Yamagishi T, Matsui M, Sekizuka T, Ito H, Fukusumi M, Uehira T, Tsubokura M, Ogawa Y, Miyamoto A, Nakamori S, Tawa A, Yoshimura T, Yoshida H, Hirokawa H, Suzuki S, Matsui T, Shibayama K, Kuroda M, Oishi K. 2020. A prolonged multispecies outbreak of IMP-6 carbapenemase-producing *Enterobacterales* due to horizontal transmission of the IncN plasmid. *Sci Rep* 10:4149. <https://doi.org/10.1038/s41598-020-60659-2>.
- Mathers AJ, Peirano G, Pitout JDD. 2015. The role of epidemic resistance plasmids and international high-risk clones in the spread of multidrug-resistant *Enterobacteriaceae*. *Clin Microbiol Rev* 28:565–591. <https://doi.org/10.1128/CMR.00116-14>.
- Harris PNA, Alexander MW. 2020. Beyond the core genome: tracking plasmids in outbreaks of multidrug-resistant bacteria. *Clin Infect Dis* <https://academic.oup.com/cid/advance-article/doi/10.1093/cid/ciaa052/5817044>. Accessed 23 June 2020.
- Yamamoto N, Asada R, Kawahara R, Hagiya H, Akeda Y, Shanmugakani RK, Yoshida H, Yukawa S, Yamamoto K, Takayama Y, Ohnishi H, Taniguchi T, Matsuoka T, Matsunami K, Nishi I, Kase T, Hamada S, Tomono K. 2017. Prevalence of, and risk factors for, carriage of carbapenem-resistant *Enterobacteriaceae* among hospitalized patients in Japan. *J Hosp Infect* 97:212–217. <https://doi.org/10.1016/j.jhin.2017.07.015>.
- Kayama S, Shigemoto N, Kuwahara R, Oshima K, Hirakawa H, Hisatsune J, Jove T, Nishio H, Yamasaki K, Wada Y, Ueshimo T, Miura T, Sueda T, Onodera M, Yokozaki M, Hattori M, Ohge H, Sugai M. 2015. Complete nucleotide sequence of the IncN plasmid encoding IMP-6 and CTX-M-2 from emerging carbapenem-resistant *Enterobacteriaceae* in Japan. *Antimicrob Agents Chemother* 59:1356–1359. <https://doi.org/10.1128/AAC.04759-14>.
- Abe R, Akeda Y, Sakamoto N, Kumwenda G, Sugawara Y, Yamamoto N, Kawahara R, Tomono K, Fujino Y, Hamada S. 2020. Genomic characterization of a novel plasmid carrying *bla*_{IMP-6} of carbapenem-resistant *Klebsiella pneumoniae* isolated in Osaka. *J Glob Antimicrob Resist* 21: 195–199. <https://doi.org/10.1016/j.jgar.2019.10.003>.
- Weingarten RA, Johnson RC, Conlan S, Ramsburg AM, Dekker JP, Lau AF, Khil P, Odom RT, Deming C, Park M, Thomas PJ, Henderson DK, Palmore TN, Segre JA, Frank KM. 2018. Genomic analysis of hospital plumbing reveals diverse reservoir of bacterial plasmids conferring carbapenem resistance. *mBio* 9:e02011-17. <https://doi.org/10.1128/mBio.02011-17>.
- Liu L, Feng Y, Long H, McNally A, Zong Z. 2018. Sequence type 273 carbapenem-resistant *Klebsiella pneumoniae* carrying *bla*_{NDM-1} and *bla*_{IMP-4}. *Antimicrob Agents Chemother* 62:e00161-18. <https://doi.org/10.1128/AAC.00160-18>.
- Yang L, Lin Y, Lu L, Xue M, Ma H, Guo X, Wang K, Li P, Du X, Qi K, Li Peng SH. 2020. Coexistence of two *bla*_{NDM-5} genes carried on IncX3 and IncFII plasmids in an *Escherichia coli* isolate revealed by Illumina and Nanopore sequencing. *Front Microbiol* 11:195. <https://doi.org/10.3389/fmicb.2020.00195>.
- Rahube TO, Viana LS, Koraimann G, Yost CK. 2014. Characterization and comparative analysis of antibiotic resistance plasmids isolated from a wastewater treatment plant. *Front Microbiol* 5:558. <https://doi.org/10.3389/fmicb.2014.00558>.
- Nikaido H. 2003. Molecular basis of bacterial outer membrane permeability revisited. *Microbiol Mol Biol Rev* 67:593–656. <https://doi.org/10.1128/mmr.67.4.593-656.2003>.
- Yano H, Kuga A, Okamoto R, Kitasato H, Kobayashi T, Inoue M. 2001. Plasmid-encoded metallo-beta-lactamase (IMP-6) conferring resistance to carbapenems, especially meropenem. *Antimicrob Agents Chemother* 45:1343–1348. <https://doi.org/10.1128/AAC.45.5.1343-1348.2001>.
- Wick RR, Schultz MB, Zobel J, Holt KE. 2015. Bandage: interactive visualization of de novo genome assemblies. *Bioinformatics* 31:3350–3352. <https://doi.org/10.1093/bioinformatics/btv383>.
- Huang T-W, Chen T-L, Chen Y-T, Lauderdale T-L, Liao T-L, Lee Y-T, Chen CP, Liu YM, Lin AC, Chang YH, Wu KM, Kirby R, Lai JF, Tan MC, Siu LK, Chang CM, Fung CP, Tsai SF. 2013. Copy number change of the NDM-1 sequence in a multidrug-resistant *Klebsiella pneumoniae* clinical isolate. *PLoS One* 8:e62774. <https://doi.org/10.1371/journal.pone.0062774>.
- Rodriguez M, Holcik M, Iyer VN. 1995. Lethality and survival of *Klebsiella oxytoca* evoked by conjugative IncN group plasmids. *J Bacteriol* 177: 6352–6361. <https://doi.org/10.1128/jb.177.22.6352-6361.1995>.
- Sherry NL, Lane CR, Kwong JC, Schultz M, Sait M, Stevens K, Ballard S, Goncalves da SA, Seemann T, Gorrie CL, Stinear TP, Williamson DA, Brett J, van Diemen A, Easton M, Howden BP. 2019. Genomics for molecular epidemiology and detecting transmission of carbapenemase-producing *Enterobacterales* in Victoria, Australia, 2012 to 2016. *J Clin Microbiol* 57:9. <https://doi.org/10.1128/JCM.00573-19>.
- Zhang X, Chen D, Xu G, Huang W, Wang X. 2018. Molecular epidemiology and drug resistant mechanism in carbapenem-resistant *Klebsiella pneumoniae* isolated from pediatric patients in Shanghai, China. *PLoS One* 13:e0194000. <https://doi.org/10.1371/journal.pone.0194000>.
- Hayakawa K, Miyoshi-Akiyama T, Kirikae T, Nagamatsu M, Shimada K, Mezaki K, Sugiki Y, Kuroda E, Kubota S, Takeshita N, Kutsuna S, Tojo M, Ohmagari N. 2014. Molecular and epidemiological characterization of IMP-type metallo-beta-lactamase-producing *Enterobacter cloacae* in a large tertiary care hospital in Japan. *Antimicrob Agents Chemother* 58:3441–3450. <https://doi.org/10.1128/AAC.02652-13>.
- Ohno Y, Nakamura A, Hashimoto E, Matsutani H, Abe N, Fukuda S, Hisashi K, Komatsu M, Nakamura F. 2017. Molecular epidemiology of carbapenemase-producing *Enterobacteriaceae* in a primary care hospital in Japan, 2010–2013. *J Infect Chemother* 23:224–229. <https://doi.org/10.1016/j.jiac.2016.12.013>.
- Nicoloff H, Hjort K, Levin BR, Andersson DI. 2019. The high prevalence of antibiotic heteroresistance in pathogenic bacteria is mainly caused by gene amplification. *Nat Microbiol* 4:504–514. <https://doi.org/10.1038/s41564-018-0342-0>.

27. Andersson DI, Hughes D. 2010. Antibiotic resistance and its cost: is it possible to reverse resistance? *Nat Rev Microbiol* 8:260–271. <https://doi.org/10.1038/nrmicro2319>.
28. Bertini A, Poirel L, Bernabeu S, Fortini D, Villa L, Nordmann P, Carattoli A. 2007. Multicopy *bla*_{OXA-58} gene as a source of high-level resistance to carbapenems in *Acinetobacter baumannii*. *Antimicrob Agents Chemother* 51:2324–2328. <https://doi.org/10.1128/AAC.01502-06>.
29. Sakamoto N, Akeda Y, Sugawara Y, Takeuchi D, Motooka D, Yamamoto N, Laolerd W, Santanirand P, Hamada S. 2018. Genomic characterization of carbapenemase-producing *Klebsiella pneumoniae* with chromosomally carried *bla*_{NDM-1}. *Antimicrob Agents Chemother* 62:e01520-18. <https://doi.org/10.1128/AAC.01520-18>.
30. Watanabe M, Iyobe S, Inoue M, Mitsuhashi S. 1991. Transferable imipenem resistance in *Pseudomonas aeruginosa*. *Antimicrob Agents Chemother* 35:147–151. <https://doi.org/10.1128/aac.35.1.147>.
31. Bandoh K, Watanabe K, Muto Y, Tanaka Y, Kato N, Ueno K. 1992. Conjugal transfer of imipenem resistance in *Bacteroides fragilis*. *J Antibiot* 45:542–547. <https://doi.org/10.7164/antibiotics.45.542>.
32. Osano E, Arakawa Y, Wacharotayankun R, Ohta M, Horii T, Ito H, Yoshimura F, Kato N. 1994. Molecular characterization of an enterobacterial metallo beta-lactamase found in a clinical isolate of *Serratia marcescens* that shows imipenem resistance. *Antimicrob Agents Chemother* 38:71–78. <https://doi.org/10.1128/aac.38.1.71>.
33. Kurokawa H, Yagi T, Shibata N, Shibayama K, Arakawa Y. 1999. World-wide proliferation of carbapenem-resistant gram-negative bacteria. *Lancet* 354:955. [https://doi.org/10.1016/S0140-6736\(05\)75707-X](https://doi.org/10.1016/S0140-6736(05)75707-X).
34. Aoki K, Harada S, Yahara K, Ishii Y, Motooka D, Nakamura S, Akeda Y, Iida T, Tomono K, Iwata S, Moriya K, Tateda K. 2018. Molecular characterization of IMP-1-producing *Enterobacter cloacae* complex isolates in Tokyo. *Antimicrob Agents Chemother* 62:e02091-17. <https://doi.org/10.1128/AAC.02091-17>.
35. Pei Y, Terajima J, Saito Y, Suzuki R, Takai N, Izumiya H, Morita-Ishihara T, Ohnishi M, Miura M, Iyoda S, Mitobe J, Wang B, Watanabe H. 2008. Molecular characterization of enterohemorrhagic *Escherichia coli* O157:H7 isolates dispersed across Japan by pulsed-field gel electrophoresis and multiple-locus variable-number tandem repeat analysis. *Jpn J Infect Dis* 61:58–64.
36. Clinical and Laboratory Standards Institute. 2020. M100 performance standards for antimicrobial susceptibility testing, 28th ed. Clinical and Laboratory Standards Institute, Wayne, PA. <http://file.qums.ac.ir/repository/mmrc/CLSI-2018-M100-S28.pdf>. Accessed 21 May 2020.
37. Wick RR, Judd LM, Gorrie CL, Holt KE. 2017. Unicycler: resolving bacterial genome assemblies from short and long sequencing reads. *PLoS Comput Biol* 13:e1005595. <https://doi.org/10.1371/journal.pcbi.1005595>.
38. Koren S, Walenz BP, Berlin K, Miller JR, Bergman NH, Phillippy AM. 2017. Canu: scalable and accurate long-read assembly via adaptive k-mer weighting and repeat separation. *Genome Res* 27:722–736. <https://doi.org/10.1101/gr.215087.116>.
39. Kolmogorov M, Yuan J, Lin Y, Pevzner PA. 2019. Assembly of long, error-prone reads using repeat graphs. *Nat Biotechnol* 37:540–546. <https://doi.org/10.1038/s41587-019-0072-8>.
40. Walker BJ, Abeel T, Shea T, Priest M, Abouelliel A, Sakthikumar S, Cuomo CA, Zeng Q, Wortman J, Young SK, Earl AM. 2014. Pilon: an integrated tool for comprehensive microbial variant detection and genome assembly improvement. *PLoS One* 9:e112963. <https://doi.org/10.1371/journal.pone.0112963>.
41. Vaser R, Sovic I, Nagarajan N, Sikic M. 2017. Fast and accurate *de novo* genome assembly from long uncorrected reads. *Genome Res* 27:737–746. <https://doi.org/10.1101/gr.214270.116>.
42. Carattoli A, Zankari E, Garcia-Fernandez A, Voldby Larsen M, Lund O, Villa L, Moller AF, Hasman H. 2014. In silico detection and typing of plasmids using PlasmidFinder and plasmid multilocus sequence typing. *Antimicrob Agents Chemother* 58:3895–3903. <https://doi.org/10.1128/AAC.02412-14>.
43. Zankari E, Hasman H, Cosentino S, Vestergaard M, Rasmussen S, Lund O, Aarestrup FM, Larsen MV. 2012. Identification of acquired antimicrobial resistance genes. *J Antimicrob Chemother* 67:2640–2644. <https://doi.org/10.1093/jac/dks261>.
44. Siguier P, Perochon J, Lestrade L, Mahillon J, Chandler M. 2006. ISfinder: the reference centre for bacterial insertion sequences. *Nucleic Acids Res* 34:D32–D36. <https://doi.org/10.1093/nar/gkj014>.
45. Brettin T, Davis JJ, Disz T, Edwards RA, Gerdes S, Olsen GJ, Olson R, Overbeek R, Parrello B, Pusch GD, Shukla M, Thomason JA, Stevens R, Vonstein V, Wattam AR, Xia F. 2015. RASTtk: a modular and extensible implementation of the RAST algorithm for building custom annotation pipelines and annotating batches of genomes. *Sci Rep* 5:8365. <https://doi.org/10.1038/srep08365>.
46. Sullivan MJ, Petty NK, Beatson SA. 2011. Easyfig: a genome comparison visualizer. *Bioinformatics* 27:1009–1010. <https://doi.org/10.1093/bioinformatics/btr039>.
47. Ma L, Ishii Y, Ishiguro M, Matsuzawa H, Yamaguchi K. 1998. Cloning and sequencing of the gene encoding Toho-2, a class A beta-lactamase preferentially inhibited by tazobactam. *Antimicrob Agents Chemother* 42:1181–1186. <https://doi.org/10.1128/AAC.42.5.1181>.
48. Schmittgen TD, Livak KJ. 2008. Analyzing real-time PCR data by the comparative *CT* method. *Nat Protoc* 3:1101–1108. <https://doi.org/10.1038/nprot.2008.73>.
49. Stoesser N, Sheppard AE, Peirano G, Sebra R, Lynch T, Anson L, Kasarskis A, Motyl MR, Crook DW, Pitout JD. 2016. Complete sequencing of plasmids containing *bla*_{OXA-163} and *bla*_{OXA-48} in *Escherichia coli* sequence type 131. *Antimicrob Agents Chemother* 60:6948–6951. <https://doi.org/10.1128/AAC.01130-16>.